# Critical behavior of the three-dimensional site-random Ising magnet: $Mn_xZn_{1-x}F_2$

P. W. Mitchell* and R. A. Cowley
*Department of Physics, University of Edinburgh, Edinburgh EH9 3JZ, Scotland*

H. Yoshizawa
*Institute for Solid State Physics, University of Tokyo, Roppongi, Minato-ku, Tokyo 106, Japan*

P. Böni and Y. J. Uemura
*Department of Physics, Brookhaven National Laboratory, Upton, New York 11973*

R. J. Birgeneau
*Department of Physics, Massachusetts Institute of Technology, Cambridge, Massachusetts 02139*
(Received 27 March 1986)

Neutron scattering has been used to study the critical behavior of the site-random Ising system, $Mn_xZn_{1-x}F_2$, for $x=0.75$ and 0.50. With the $x=0.75$ sample, which is of particularly high quality, measurements were possible over nearly three decades, $4\times10^{-4}<|t|<2\times10^{-1}$ both above and below $T_N$; the resulting exponents are $\nu=\nu'=0.715\pm0.035$ and $\gamma=\gamma'=1.364\pm0.076$, and the corresponding amplitude ratios are $0.69\pm0.02$ and $2.45\pm0.15$, respectively. These agree well with values obtained in $Fe_xZn_{1-x}F_2$ for $x=0.46$ and 0.50 and with theoretical predictions for the random exchange Ising model. With the $x=0.5$ sample, high-energy resolution scans were carried out in the critical region below $T_N$; these experiments indicate that the predicted elastic Lorentzian-squared scattering is too small in magnitude to be measured and specifically that it does not affect the amplitude ratios given above.

## I. INTRODUCTION

The properties of the phase transitions of disordered systems have been the subject of a great deal of recent work. In systems with random exchange constants, Harris[1] predicted that the critical behavior of the random system would be similar to that of the pure system if the specific-heat exponent $\alpha$ were less than zero. If $\alpha$ is greater than zero, new behavior is to be expected. Among the $n$-vector models in $d=3$ dimensions, only the Ising model has $\alpha>0$, and the corresponding new critical behavior has been obtained as an unusual fixed point dependent upon $\sqrt{\epsilon}$ where $\epsilon=4-d$.[2-6] Experimentally these predictions are difficult to test because critical behavior can be determined only close to $T_c$, and macroscopic fluctuations in the concentration of the random system necessarily lead to a smearing of $T_c$. Suitable samples must have the different components randomly distributed but nevertheless statistically uniform on a macroscopic scale. Because of this difficulty, the interpretation of the first experiments[7,8] to test this behavior was ambiguous.

In the past few years there has, however, been a great improvement in the quality of the single crystals of the transition-metal fluorides of the rutile structure, and this has enabled a detailed study to be made of the random Ising behavior in $Fe_xZn_{1-x}F_2$.[9] The results showed that the random system did indeed have different critical exponents from those of pure $FeF_2$, and more strikingly, that the amplitude ratios were very different from those of the pure Ising fixed point.

In this paper we report on similar neutron scattering measurements for another $d=3$ Ising system, $Mn_xZn_{1-x}F_2$. There are four reasons why we have chosen to study this system. First, the critical phenomena in $MnF_2$ have been studied in detail,[10,11] and the magnetic interactions are very well understood. The interactions are largely between the nearest antiferromagnetic neighbors and those of Heisenberg character, but the weaker dipolar interactions break the rotational symmetry. It is therefore an example of a system with weak Ising anisotropy, in contrast to $FeF_2$, which has a very large Ising anisotropy of crystal-field origin.[12] Second, since the crossover from pure Ising behavior to random Ising behavior is determined[2,3] by $(\Delta J/\bar{J})^{1/\alpha}$, where $\alpha$ is small, it was anticipated that the random behavior would only be observable very close to $T_N$. Surprisingly, the random Ising behavior was observed[9] over a wide temperature interval extending out to a reduced temperature of $\sim10^{-1}$ in the $Fe_{0.5}Zn_{0.5}F_2$ experiment.[9] Thus experiments on different systems and with varying concentrations are required. Third, following the work of Grinstein *et al.*,[13] Pelcovits and Aharony[14] have shown, for $T<T_N$, that the scattering cross section contains, in addition to the usual susceptibility and Bragg terms, a contribution to the diffuse scattering from the random static ordered moments; this term must be included in line-shape analysis and in comparison of the measured amplitude ratios with theory. Fourth, the crystals used in this study have also been used for a study of the effect of random fields.[15,16] It is therefore essential to ensure that the zero-field properties are well characterized in any detailed study of the

 ©1986 The American Physical Society

random-field effects.

In the next section the experimental techniques are described; the data analysis is given in Sec. III. The conclusions are given in the final section.

## II. EXPERIMENTAL TECHNIQUES

Two single crystals of $Mn_xZn_{1-x}F_2$ were grown at the Massachusetts Institute of Technology by D. Gabbe and A. Linz using the Czochralski method with $x$ nominally 0.75 and 0.5. The growth direction was the $a$ axis for the $x=0.75$ sample and the $c$ axis for the $x=0.5$ sample. In both cases the virgin boules were approximately cylindrical, 2 cm in height and 2 cm in diameter. For the random-field and critical-scattering measurements, small samples were cut out of the center portion of the boules. Typical dimensions of the illuminated volume were $4\times6\times6$ mm$^3$. The crystals were of excellent crystallographic quality and had a mosaic spread of less than 0.02°. No evidence was found for any chemical ordering of the Mn and Zn ions and so the samples are excellent examples of a site-random system. The measurements are limited by macroscopic, nonstatistical concentration fluctuations; these are best characterized by the sharpness of the phase transition itself. In neutron experiments, concentration fluctuations manifest themselves both through persistence of the Bragg scattering into the paramagnetic phase and by the minimum, nonzero width of the critical scattering at $T_N$. The $x=0.75$ sample turned out to be excellent, the overall spread in concentration being less than 0.1%; we have therefore performed measurements down to $\sim4\times10^{-4}$ in reduced temperature; the $x=0.5$ sample is of lower quality with a concentration spread of at least 0.5%. The $x=0.75$ crystal was mounted with the (010) crystallographic axis vertical in a variable-temperature cryostat at the Brookhaven High-Flux Beam Reactor. The crystal could be maintained at a temperature with a stability of 0.005 K and a comparable relative accuracy and with an absolute accuracy of better than 0.05 K.

In $Mn_xZn_{1-x}F_2$ there is significant neutron scattering from both the transverse and longitudinal spin fluctuations. Consequently, in a detailed study of the phase transition it is necessary to separate these two contributions. This is accomplished[7,10] by performing measurements of the scattering around the (001) reciprocal-lattice point; the (001) response is determined almost solely by the transverse fluctuations. The scattering around the (100) reciprocal-lattice point is given by the sum of the longitudinal and transverse contributions, so that the former can be obtained by subtracting the latter, which are known from the measurements around (001).

Most of the measurements were performed with a two-axis spectrometer so as to perform the energy integration over the frequency-dependent scattering cross section experimentally. It is then essential to use an incident neutron energy which is much higher than the energy of the fluctuations if the energy or frequency dependence of the cross section is not to cause errors.[10] Most of the experiments on the $x=0.75$ sample were performed with a two-axis spectrometer with an incident neutron energy of 30.5 meV which was obtained by reflection from a pyrolytic graphite monochromator. The horizontal collimations from reactor to counter were 20′, 20′, and 20′ giving a measured resolution [half width at half maximum (HWHM)] at the (100) lattice point of 0.0015 reciprocal-lattice units (rlu) along (001), 0.011 rlu along (100), and 0.049 rlu along (010). A pyrolytic graphite filter was used to reduce the higher-order contaminant neutrons. By using this arrangement, $T_N$ was determined from the peak in the critical scattering as $46.2\pm0.1$ K, and measurements made of the diffuse scattering near (100) and (001) reciprocal-lattice points at 36 temperatures between 55 and 37 K.

Some scans were performed with higher resolution with an incident neutron energy of 14 meV and collimation of 20′, 10′, and 5′ from reactor to counter. The measured resolution (HWHM) at the (100) lattice point was then 0.00061 rlu along (001), 0.0089 rlu along (100), and 0.042 rlu along (010), and 18 different temperatures were studied above and below $T_N$.

A number of independent experiments were performed on the $x=0.5$ material. First, a series of experiments utilizing a triple-axis spectrometer set to zero energy transfer with very good energy resolution were carried out on the full 8-cm$^3$ boule before cutting. As we shall discuss below, the square of the Lorentzian scattering below $T_N$ should be purely elastic since it originates from the static random ordered moments. Measurements were carried out with an incident neutron energy of 3.5 meV and collimation such that the energy resolution (HWHM) was 0.040 meV, as well as with an incident energy of 13.7 meV when the energy resolution was 0.15 meV.

The critical scattering measurements, all of which utilized a two-axis spectrometer, were carried out on a piece of the $x=0.5$ crystal of dimensions $1\times0.5\times0.5$ cm$^3$ with the $c$ axis along the 1-cm direction. In the first set of measurements on this sample, the crystal was mounted with an $a$ axis vertical in a temperature-controlled cryostat. Survey measurements were carried out at with an incident neutron energy of 13.7 meV, and all collimation 10′, to assess the transverse susceptibility, $\chi_T(q)$. As part of a study of random-field effects the sample was then mounted with the $c$ axis vertical in a superconducting magnet; the bottom 6 mm were masked with cadmium in order to reduce the overall concentration spread. In this configuration, measurements were made of the combination $\chi_L+\chi_T$, by using a two-axis spectrometer with an incident energy of 13.7 meV, and all 10′ collimators. The wave-vector resolution elements in the order given above were 0.0013, 0.007, and 0.07 rlu.

## III. RESULTS AND ANALYSIS

We discuss first the quasielastic scattering below $T_N$ from the $x=0.5$ sample. As noted by Grinstein *et al.*[13] and as developed by Pelcovits and Aharony,[14] below $T_N$ in a random magnet one expects, in addition to the normal Bragg scattering and Lorentzian diffuse scattering, a higher-order term in the longitudinal cross section:

$$C^{(s)}(\mathbf{q})=\chi_L^2(\mathbf{q})D(\mathbf{q}) , \quad (1)$$

where $\chi_L(\mathbf{q})$ is the longitudinal wave-vector-dependent susceptibility and $D(\mathbf{q})$ is a wave-vector-dependent amplitude factor. In mean-field theory $D(\mathbf{0}) \sim M_s^2$ where $M_s$ is the sublattice magnetization. From a scaling analysis,[14] it is found that in the random exchange critical regime $C^{(s)}(0) \sim |t|^{-\gamma}$. The relative amplitudes of the Lorentzian and Lorentzian-squared fluctuation terms are not currently known and hence must be determined by experiment.

This Lorentzian-squared scattering is analogous to the Lorentzian-squared term which occurs in the random-field problem.[15,16] Specifically, it can be viewed as originating from the field generated by the random component of the ordered moments. An essential feature which should distinguish the Lorentzian and Lorentzian-squared contributions is that the former is dynamic while the latter is static.[17] The same situation occurs in the random-field problem and indeed it has been shown from the random-field experiments in $Mn_xZn_{1-x}F_2$ with $x=0.50$ and 0.75, that an energy resolution of $\sim 0.1$ meV is sufficient to isolate the Lorentzian-squared component down to the 1% level in intensity.[15,16] Accordingly, the high-energy resolution experiments described in the previous section were performed.

We show in Fig. 1 scans with a triple-axis spectrometer set for $E=0$ through the (100) position at 19.0, 20.25, and 20.75 K, all below $T_N=21.0$ K for the large $x=0.50$ boule. The 19.0-K data were taken with the 0.040-meV resolution configuration, while the data at 20.25 and 20.75 K were taken with 0.15-meV resolution. From separate inelastic studies[18] it is known that at these temperatures the transverse component is eliminated by the high-energy resolution so that the measured response is purely longitudinal. The solid lines in Fig. 1 are the best fits to a pure Lorentzian while the dashed lines are the best fits to a Lorentzian squared. It is evident that, in contrast to the random-field problem there is no measurable Lorentzian-squared component. The correlation lengths obtained from the Lorentzian fits agree well with the more detailed two-axis results presented below.

The energy integrated intensity for a wave-vector transfer $\mathbf{Q}$ for magnetic scattering by $Mn_xZn_{1-x}F_2$ thus may be taken as

$$I(\mathbf{Q}) = C\,|f(\mathbf{Q})|^2 T[(\sin^2\theta)\chi_L(\mathbf{q}) + (1+\cos^2\theta)\chi_T(\mathbf{q})] + D\,|f(\mathbf{Q})|^2(\sin^2\theta)M_s^2\delta(\mathbf{q}), \quad (2)$$

where $f(\mathbf{Q})$ is the form factor of the $Mn^{2+}$ ion, $\chi_L(\mathbf{q})$ and $\chi_T(\mathbf{q})$ are the longitudinal and transverse wave-vector-dependent susceptibilities, respectively, and $\mathbf{Q}=\mathbf{q}+\mathbf{G}$ where $\mathbf{G}$ is an antiferromagnetic reciprocal-lattice vector. $T$ is the absolute temperature, $C$ and $D$ are constants, $M_s$ is the ordered staggered moment occurring below $T_N$, and $\theta$ is the angle between $\mathbf{Q}$ and the crystallographic $c$ axis.

We present now the double-axis results in the $x=0.75$ sample. As discussed in the preceding section, data were taken around both the (001) and (100) reciprocal-lattice positions. Initially, the data taken near the (001) reciprocal-lattice point were analyzed using Eq. (2) and assuming that $\theta=0$ so that there was no contribution from $\chi_L$ and $M_s^2$. The transverse susceptibility was then assumed to be of Lorentzian form and isotropic in reciprocal space with

$$\chi_T(\mathbf{q}) = \frac{A_T}{K_T^2 + (\mathbf{q}^*)^2}, \quad (3)$$

where

$$\mathbf{q}^* = \left[\frac{2\pi}{a}q_x, \frac{2\pi}{a}q_y, \frac{2\pi}{c}q_z\right].$$

$K_T$ and $A_T$ were then determined as functions of temperature by fitting Eq. (3) convoluted with the experimental resolution function plus a background to the observable data. At each temperature a good fit ($\chi^2 < 1.5$) was obtained. The results for $K_T$ are illustrated in Fig. 2 and show that on decreasing the temperature, $K_T$ decreases as

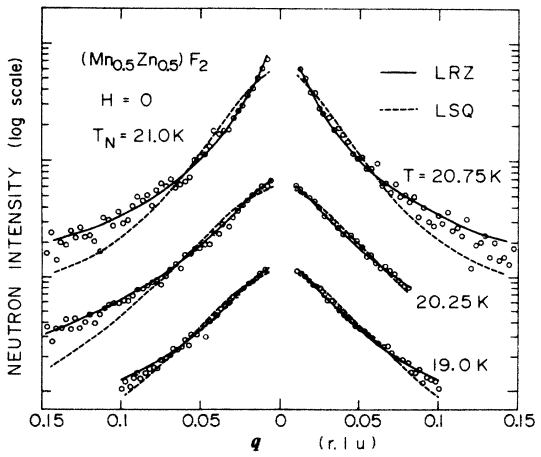


FIG. 1. High-energy resolution transverse scans through (1,0,0) Bragg reflection in $Mn_{0.5}Zn_{0.5}F_2$. The resolution function and fits are discussed in the text.

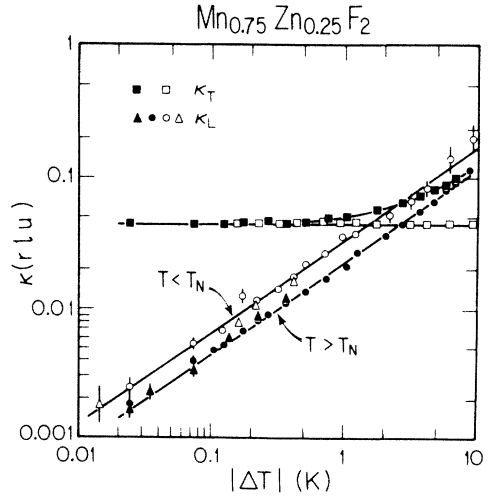


FIG. 2. Transverse and longitudinal inverse correlation lengths in $Mn_{0.75}Zn_{0.25}F_2$. The solid points are above $T_N$ while the open points are below $T_N$. Open and solid triangles represent points taken with $E_i=14$ meV.

$T_N$ is approached but is finite at $T_N$, and then is almost independent of temperature below $T_N$. For the sample with $x=0.75$, $K_T$ decreases as $T_N$ is approached to a value of $0.043\pm0.001$ rlu at $T_N$ and then is almost independent of temperature below $T_N$. The amplitude $A_T$ (not shown) decreases both above and below $T_N$. Above $T_N$, $TA_T$ is constant to within the experimental error while below $T_N$, $TA_T$ decreases by $\sim 15\%$ between $T_N$ and 37.0 K.

Once the behavior of the transverse fluctuations had been determined, the longitudinal fluctuations could be obtained from the measurements taken near the (100) reciprocal-lattice point. Representative $(1,0,\zeta)$ scans are shown in Fig. 3. In principle it should be possible to subtract the transverse intensity at (100) by dividing the intensity observed at (001) by one-half ($\theta$ factor) and multiplying by the ratio of the form factors $|f(\mathbf{G}=(1,0,0))|^2/|f(\mathbf{G}=(0,0,1))|^2$. Although this gives approximately the correct scale factor, the crystals are not of a symmetric shape, and the scattering angles and hence absorption corrections differ so that the real scale factor may be different from the calculated value. We determine the scale factor from measurements at high temperatures where we assume that longitudinal and transverse susceptibilities are equal and at low temperatures where the longitudinal susceptibility is zero. These experiments gave a scale factor by which the data taken near the (001) point should be scaled to obtain the transverse scattering near the (100) point; this scale factor was within 10% of the theoretical value. This ratio was then used in the data analysis.

The data analysis was then performed by assuming that

$$\chi_L(\mathbf{q})=\frac{A_L}{K_L^2+(\mathbf{q}^*)^2}\ , \tag{4}$$

and fitting $A_L$, $K_L$, and $M_s^2$ to the experimental data while holding $A_T$ and $K_T$ fixed. A good fit was obtained both above and below $T_N$ with typically $\chi^2<2.0$ (see Fig. 3) except for data taken at high temperatures $>50$ K and low temperature $<40$ K, for which $\chi^2$ increased. These increased errors are caused at least in part by the very small contribution of the longitudinal scattering at low temperatures and at high temperatures by the effects of higher-order contamination in the incident neutron beam.

The results for $K_L$ are shown in Fig. 2, whereas those for $A_L$ are shown in the form of the susceptibility $\chi_L=A_L/K_L^2$ in Fig. 4. It should be noted from Figs. 2 and 4 that it was possible to obtain reliable data for temperatures as close as 0.02 K to the critical point ($|t|=|T/T_N-1|=4\times10^{-4}$) and for inverse correlation lengths as small as $\sim 0.0015$ rlu although these are at the limits of our present sample. This demonstrates that this $Mn_{0.75}Zn_{0.25}F_2$ sample is remarkably homogeneous with the Mn and Zn atoms distributed statistically on both microscopic and macroscopic length scales. This also suggests that the transition widths in the random-field experiments[15] are intrinsic.

These results were fitted to obtain the exponents and

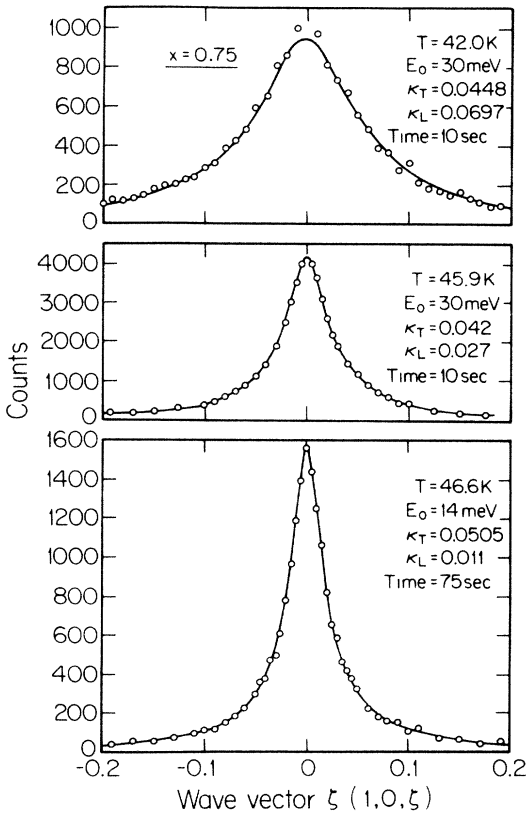


FIG. 3. Representative transverse scans through the (100) Bragg reflection at the temperatures indicated. The solid lines represent fits to Eq. (3) with the parameters given in the figure.

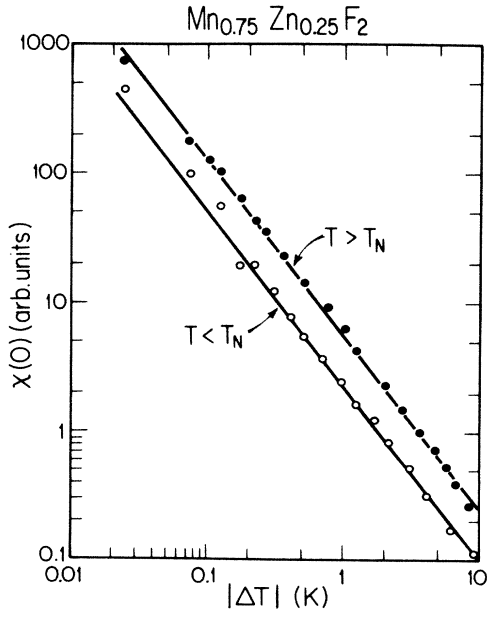


FIG. 4. The susceptibility $\chi(0)$ in $Mn_{0.75}Zn_{0.25}F_2$; the solid lines are the results of fits to single power laws with exponent $\sim 1.364$ above and below $T_N$.

amplitude ratios:

$$K_L(T)=\begin{cases}K_L^+(T-T_N)^\nu, & T>T_N\\ K_L^-(T_N-T)^\nu, & T<T_N\end{cases}, \quad (5)$$

and

$$\chi_L(T)=\begin{cases}C_L^+(T-T_N)^{-\gamma}, & T>T_N\\ C_L^-(T_N-T)^{-\gamma}, & T<T_N\end{cases}. \quad (6)$$

Initially fits were performed by varying the amplitudes, exponents, and $T_N$ and a variety of fits were performed with different sets of data and different fitting parameters. The results were all consistent with $\nu$ and $\gamma$ determined from data above and below $T_N$ being the same; the resulting best values of the parameters are shown in Table I. The statistical error limits are quite small; the errors given in Table I represent our best estimate of the overall uncertainties including systematic effects.

The fits also provided values of the ordered moment $M_s^2$ below $T_N$ but the crystals are crystallographically very perfect and so extinction occurs even close to $T_N$; thus the data do not give satisfactory values of the order-parameter exponent $\beta$. $\beta$ has been determined by Dunlap and Gottlieb[20] in $Mn_{0.86}Zn_{0.14}F_2$ to be $0.349\pm0.008$, in agreement with the random Ising value.[5,6]

As a cross check on our inelastic results in the $x=0.5$ sample we also performed fits of the $x=0.75$ data for $T<T_N$ to a Lorentzian plus Lorentzian-squared form. For all but one temperature point, $\chi^2$ was reduced by 0.02 or less by including the Lorentzian-squared term and further, the amplitude of the Lorentzian squared was within error zero for each of these temperatures. Only for one temperature, 46.15 K, was $\chi^2$ decreased significantly. However, we suspect that this result arises from the difficulty of separating Bragg, Lorentzian, and Lorentzian-squared components very close to $T_N$, where $K_L$ is small.

The critical scattering experiments in the small $x=0.5$ sample were rather less satisfactory. These were performed as an ancillary part of a study of random-field effects in this material and were carried out primarily to characterize the zero-field behavior. Because of the larger concentration spread, measurements were only possible 0.1 K and further away from $T_N=20.72$ K corresponding to reduced temperatures of $5\times10^{-3}$ and greater. As discussed in Sec. II, initial measurements were carried out using a two-axis spectrometer illuminating the whole sample in a conventional cryostat and with an $a$ axis vertical so that (001) and (100) reflections could be accessed. These measurements gave $K_T=0.062\pm0.08$ rlu for $|T-T_N|\leq 2$ K and $A_T\simeq 0.7A_L$; it was also found that $A_L$ was a minimum at $T_N$ implying $\eta>0$ as expected.

More detailed measurements were carried out on the masked crystal mounted with the $c$ axis vertical in a superconducting magnet, again utilizing a two-axis spectrometer as discussed in the preceding section. In this case $\chi_T$ could not be measured directly, but only the combination $\chi_L+\chi_T$. In order to analyze the data we assumed the above value $K_T=0.062$ rlu and the ratio $A_T/A_L=0.7$. The data were then fitted to Eq. (2) excluding the center portion of the scans. The results so obtained for $K_L$ and $\chi_L$ above and below $T_N$ are shown in Figs. 5 and 6, respectively. Reasonable power laws are obtained over about one decade; further, the data give $\nu=\nu'$ and $\gamma=\gamma'$ within the errors. The best-fit exponents are listed in Table I. They are rather larger than those in $Mn_{0.75}Zn_{0.25}F_2$ although the results agree within the combined uncertainties. Here the primary uncertainty arises from the subtraction of $\chi_T$, which is not measured directly; the fact that this latter experiment gives $\gamma>2\nu$ whereas the preliminary results had $\gamma<2\nu$ shows that there must be some small systematic errors. This small error leads to a remarkably large increase in the effective $\gamma$. The ratios $K_L^+/K_L^-$ and $\chi_L^+/\chi_L^-$ may, however, be measured much more accurately since near $T_N$ they are insensitive to an error in the $\chi_T$ subtraction. We list in Table I these ratios extracted from the data for less than

TABLE I. Exponents and amplitude ratios in diluted Ising antiferromagnets.

| | $\nu$ | $\nu'$ | $K/K'$ | $\gamma$ | $\gamma'$ | $\chi/\chi'$ | Range |
|---|---|---|---|---|---|---|---|
| $Mn_{0.75}Zn_{0.25}F_2$[a] | 0.715±0.035[b] | 0.715±0.035[b] | 0.71±0.02 | 1.364±0.076[b] | 1.364±0.076[b] | 2.56±0.15 | $4\times10^{-4}<\lvert t\rvert<2\times10^{-1}$ |
| $Mn_{0.5}Zn_{0.5}F_2$[c] | 0.75±0.05 | 0.76±0.08 | 0.65±0.05 | 1.57±0.16 | 1.56±0.16 | 2.2±0.2 | $5\times10^{-3}<\lvert t\rvert<10^{-1}$ |
| $Fe_{0.46}Zn_{0.54}F_2$[d] | 0.69±0.01[b] | 0.69±0.01[b] | 0.69±0.02 | 1.31±0.03[b] | 1.31±0.03[b] | 2.8±0.4 | $1.5\times10^{-3}<\lvert t\rvert<10^{-1}$ |
| $Fe_{0.5}Zn_{0.5}F_2$[e] | 0.74±0.03 | 0.72±0.03 | 0.73±0.02 | 1.45±0.06 | 1.43±0.06 | 2.2±0.11 | $2\times10^{-3}<\lvert t\rvert<10^{-1}$ |
| Averaged values | 0.71±0.02 | | 0.70±0.02 | 1.37±0.04 | | 2.4±0.02 | |
| Theory[f] | 0.70<br>0.69 | | 0.83 | 1.39<br>1.34 | | 2.2 | |

[a]Values obtained in this work.
[b]The exponents $\nu,\nu'$, and $\gamma,\gamma'$ have been kept equal during the final fitting procedure.
[c]Values obtained in this work.
[d]Reference 19.
[e]Reference 9.
[f]Reference 5, A. Newlove, J. Phys. C 16, L423 (1983).

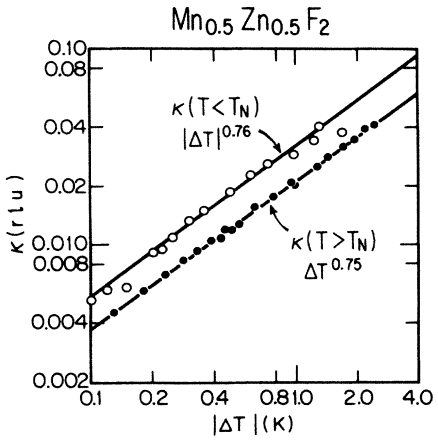


FIG. 5. Inverse correlation length above and below $T_N$ in $Mn_{0.5}Zn_{0.5}F_2$.

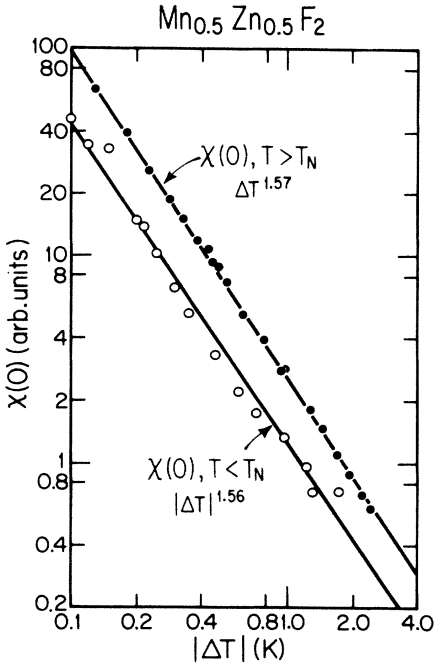


FIG. 6. The susceptibility $\chi(0)$ in $Mn_{0.5}Zn_{0.5}F_2$.

$10^{-2}$ in reduced temperature. As may be seen from the table, the ratios in each of the $Mn_xZn_{1-x}F_2$ and $Fe_xZn_{1-x}F_2$ samples agree very well.

## IV. CONCLUSIONS

As discussed above, we have obtained accurate values for the exponents and amplitude ratios over nearly three decades above and below $T_N$ in the site-random Ising antiferromagnet $Mn_{0.75}Zn_{0.25}F_2$. We have also obtained reliable values for the amplitude ratios in $Mn_{0.5}Zn_{0.5}F_2$. These are tabulated in Table I together with corresponding results in $Fe_xZn_{1-x}F_2$, $x=0.50$ and 0.46, and the current theoretical predictions. For purposes of comparison we have compiled in Table II corresponding results in the pure systems $MnF_2$ and $FeF_2$. In Table I we give averaged values for all current measurements: $\nu=\nu'=0.71\pm0.02$, $K^+/K^-=0.70\pm0.02$, $\gamma=\gamma'=1.37\pm0.04$, and $\chi^+/\chi^-=2.4\pm0.2$. In computing these averages we have excluded the $Mn_{0.5}Zn_{0.5}F_2$ exponents. As may be seen from Table I the agreement with current theoretical values is excellent. From the spread in the measured values in Tables I and II it is evident that systematic errors are dominant. The systematic errors originate primarily in the resolution corrections, the quasielastic approximation, concentration fluctuations, and the background correction. Finally, no correction-to-scaling terms have been used in the $Mn_xZn_{1-x}F_2$ power-law analyses so that the results correspond to effective exponents; since the correction terms have nonuniversal amplitudes this may also produce a systematic error.

Comparison with Table II shows that the critical behavior in $Mn_xZn_{1-x}F_2$ and $Fe_xZn_{1-x}F_2$ is now at least as well characterized with neutrons as in the pure materials $MnF_2$ and $FeF_2$ especially below $T_N$. In both $MnF_2$ and $FeF_2$, the experiments which extend closest to $T_N$ give good agreement with pure Ising model predictions with respect to both exponents and amplitude ratios. The spread in experimental values, however, again illustrates

TABLE II. Exponents and amplitude ratios in pure Ising antiferromagnets.

| | $\nu$ | $\nu'$ | $K/K'$ | $\gamma$ | $\gamma'$ | $\chi/\chi'$ | Range |
|---|---|---|---|---|---|---|---|
| $FeF_2$[a] | 0.67±0.04 | 0.7±0.2 | 0.5±0.1 | 1.38±0.08 | 1.6±0.2 | 6.1±1.0 | $10^{-3}<\|t\|<10^{-1}$ |
| $FeF_2$[c] | 0.64±0.01[b] | 0.64±0.01[b] | 0.53±0.01 | 1.25±0.02[b] | 1.25±0.02[b] | 4.6±0.2 | $10^{-4}<\|t\|<10^{-2}$ |
| $MnF_2$[d] | 0.63±0.04 | 0.56±0.1 | 0.59±0.09 | 1.27±0.04 | 1.32±0.12 | 4.8±1.0 | $10^{-3}<\|t\|<10^{-1}$ |
| $MnF_2$[e] | 0.68±0.06 | | | 1.35±0.02 | | | $4\times10^{-3}<\|t\|<10^{-1}$ |
| Theory[f] | 0.63 | 0.63 | 0.51 | 1.24 | 1.24 | 5.1 | |

[a]Reference 12.
[b]The exponents $\nu,\nu'$, and $\gamma,\gamma'$, have been kept equal during the final fitting procedure.
[c]Reference 22.
[d]Reference 10 (Schulhof *et al.*).
[e]Reference 10 (Dietrich); here the errors are purely statistical.
[f]References 23 and 24.

the importance of systematic versus statistical errors. It is noteworthy that the amplitude ratios change much more than the exponents themselves as one goes from pure to random Ising behavior.

The most surprising features of our results is that $Mn_{0.75}Zn_{0.25}F_2$ appears to exhibit random Ising behavior over the complete reduced temperature range $4\times10^{-4}<|t|<2\times10^{-1}$. In this system $(\Delta J/J)^{1/\alpha}\sim(\frac{1}{4})^{1/\alpha}\simeq10^{-5}$ so that according to current theoretical ideas[1-6] the random exchange critical region should have been experimentally inaccessible. Clearly this is not the case. Finally, we also did not observe the anticipated Lorentzian-squared diffuse scattering below $T_N$. The exponents obtained here are important in evaluating results in the random-field Ising model; this will be discussed in a separate paper.[21]

## ACKNOWLEDGMENTS

We are especially grateful to A. Aharony and Y. Shapira for extensive discussion of these results and to D. P. Belanger for communicating the $FeF_2$ results prior to publication. P. W. Mitchell is thankful for the hospitality of the Brookhaven National Laboratory. The work at the Massachusetts Institute of Technology was supported by the U.S. National Science Foundation Low Temperature Physics Program—Contract No. DMR85-01856, at Brookhaven by the Division of Materials Science, U.S. Department of Energy under Contract No. DE-AC02-76CN00016, and at Edinburgh by the U.K. Science and Engineering Research Council. H. Yoshizawa participated in this work under the auspices of the U.S.-Japan Cooperative Neutron Scattering Program.

---

*Present address: Department of Physics, University of Manchester, Manchester, M13 9PL, United Kingdom.

[1]A. B. Harris, J. Phys. C 7, 1671 (1974).

[2]D. E. Khmelnitskii, Zh. Eksp. Teor. Fiz. **68**, 1960 (1975) [Sov. Phys.—JETP **41**, 981 (1975)].

[3]A. B. Harris and T. C. Lubensky, Phys. Rev. Lett. **33**, 1540 (1974); G. Grinstein and A. Luther, Phys. Rev. B **13**, 1329 (1976).

[4]C. Jayaprakash and H. J. Katz, Phys. Rev. B **16**, 3987 (1977).

[5]G. Jug, Phys. Rev. **27**, 609 (1983); K. E. Newman and E. K. Riedel, Phys. Rev. B **25**, 264 (1982); I. O. Maier and A. I. Sokolov, Fiz. Tverd. Tela (Leningrad) **26**, 3454 (1984) [Sov. Phys. Solid State **26**, 2076 (1984)].

[6]M. Kaufman and M. Kardar, Phys. Rev. B **31**, 2913 (1985).

[7]G. M. Mayer and O. W. Dietrich, J. Phys. C **11**, 1451 (1978).

[8]R. A. Cowley and K. Carneiro, J. Phys. C **13**, 3281 (1980).

[9]R. J. Birgeneau, R. A. Cowley, G. Shirane, H. Yoshizawa, D. P. Belanger, A. R. King, and V. Jaccarino, Phys. Rev. B **27**, 6747 (1983).

[10]M. P. Schulhof, R. Nathans, P. Heller, and A. Linz, Phys. Rev. B **1**, 2304 (1970); *ibid.* **4**, 2254 (1971); O. Dietrich, J. Phys. C **2**, 2022 (1969).

[11]P. Heller, Phys. Rev. **146**, 403 (1966).

[12]M. T. Hutchings, M. P. Schulhof, and H. J. Guggenheim, Phys. Rev. B **13**, 3081 (1976), and references therein.

[13]G. Grinstein, S. K. Ma, and G. Mazenko, Phys. Rev. B **15**, 258 (1977).

[14]R. A. Pelcovits and A. Aharony, Phys. Rev. B **31**, 350 (1985).

[15]R. J. Birgeneau, R. A. Cowley, G. Shirane, and H. Yoshizawa, Phys. Rev. Lett. **54**, 2147 (1985), and references therein.

[16]R. A. Cowley, G. Shirane, H. Yoshizawa, and R. J. Birgeneau, in *Scaling Phenomena in Disordered Systems* (Plenum, New York, in press); R. J. Birgeneau, Y. Shapira, G. Shirane, R. A. Cowley, and H. Yoshizawa, Physica **137B**, 83 (1986).

[17]A. Aharony (private communication).

[18]Y. Uemura and R. J. Birgeneau (unpublished).

[19]D. P. Belanger, A. R. King and V. Jaccarino, Phys. Rev. B **34**, 452 (1986).

[20]R. A. Dunlap and A. M. Gottlieb, Phys. Rev. B **23**, 6106 (1981).

[21]R. A. Cowley, R. J. Birgeneau, H. Yoshizawa, and G. Shirane (unpublished).

[22]D. P. Belanger and H. Yoshizawa (unpublished). In this experiment non-Lorentzian line shapes were required to fit the data for $|t|<10^{-3}$. The power-law fits to $\chi$ for both $FeF_2$ and $Fe_{0.46}Zn_{0.54}F_2$ include a constant term to allow for non-diverging terms and the small effects of corrections to scaling.

[23]J. C. Le Guillou and J. Zinn-Justin, Phys. Rev. B **21**, 3976 (1980); A. J. Guttman, *ibid.* **33**, 5089 (1986).

[24]A. Aharony and P. C. Hohenberg, Phys. Rev. B **13**, 3081 (1976).